Structural Chemistry (2021) 32:2199–2207
https://doi.org/10.1007/s11224-021-01787-x

ORIGINAL RESEARCH

Quantum chemical investigation on D-π-A-based phenothiazine organic chromophores with spacer and electron acceptor effects for DSSCs

Anbarasan Ponnusamy Munusamy[1] · **Arunkumar Ammasi**[1] · **Shanavas Shajahan**[1] · **Tansir Ahamad**[2] · **M. A. Majeed Khan**[3]

Received: 22 February 2021 / Accepted: 20 April 2021 /

Abstract

In this work, the newly designed phenothiazine-based organic dye (PT-BTBA, PT-EBTBA, and PT-EBTEBA) derivatives were screened and investigated for dye-sensitized solar cell (DSSC) application. The literature dye of SB covers the electron-donor (D) in phenothiazine and cyanoacrylic acid in electron-acceptor (A) based on D-A structure. In order to improve the π-conjugation and acceptor group effects on the SB dye were theoretically investigated. The effect of D-π-A designed dyes on the optical absorption spectra and photovoltaic (PV) parameters was implemented by the density functional theory (DFT) and time-dependent DFT (TD-DFT) calculations. Also, the hybrid functionals were initially evaluated to establish an accurate methodology for calculating the first-singlet absorption peak of SB dye. Consequently, TD-CAM-B3LYP functional and 6-311++G(d,p) theory were well matched with the literature data. According to this result, phenothiazine-4-((7-ethynylbenzo[c][1,2,5]thiadiazol-4-yl)ethynyl)benzoic acid (PT-EBTEBA) dye has the strong group for more red-shifted and successful electron injected into the conduction band edge of TiO_2 surface. It is expected to provide some theoretical guidance on designing photosensitive with new metal-free organic dyes for use in DSSCs yielding highly efficient performance.

Keywords D-π-A configuration · DFT and TD-DFT calculations · CAM-B3LYP functional · Electronic and absorption spectra · DSSCs

Introduction

Michael Gratzel and O'Regan groups first developed the dye-sensitized solar cells (DSSCs) in 1991; they converted light energy into electricity [1]. In photovoltaic (PV) device, DSSC components were contained in the conduction band edge (CBE) of semiconductor titanium dioxide (TiO_2) surface, photoanode sensitized dyes, redox shuttle, and counter electrode, respectively [2]. Furthermore, sensitizers can be divided into two categories: (i) metal complex and (ii) metal-free organic dyes have one of the key components for high power conversion efficiency (PCE) in DSSCs. Recently, the scientific research report was conducted by PCE up to 24.2%, but the conventional electricity production process is still non-competitive [3]. Metal-free organic sensitizers contain the donor (D), π-bridge (π), and acceptor (A) (D-π-A) that have feasible flexibility for molecular proposal in DSSCs. Also, D-π-A pattern of the dyes was strongly desirable because of their several features, such as large absorption wavelength, high efficiency, tunable molecules with optoelectronic properties, lower cost large-scale production, easier preparation, and purification [4–7]. Other major advantages of the organic sensitizers cover the tunable absorption wavelength and PV properties over suitable molecular architecture [8, 9]. In literature, novel organic merocyanine [10], cyanine [11], hemicyanine [12], triphenylamine [13–16], dialkylaniline

Highlights
- The phenothiazine-based organic dyes are designed and investigated.
- The absorption wavelength of PT-EBTEBA showed better dye than the SB and other molecules.

✉ Anbarasan Ponnusamy Munusamy
profpmanbarasan@gmail.com

[1] Department of Physics, Periyar University, Salem 636 011, India

[2] Department of Chemistry, College of Science, King Saud University, P.O. Box 2455, Riyadh 11451, Saudi Arabia

[3] King Abdullah Institute for Nanotechnology, King Saud University, Riyadh 11451, Saudi Arabia

[17], phenothiazine [18], tetrahydroquinoline [19], coumarins [20–23], indoline [24–27], and carbazole [28] dyes were successfully investigated and proven for DSSC application. For example, Kar groups reported on N,N′-dialkylaniline (NDI 6)-based DSSCs that exhibit PCE up to 19.24% [29].

Highly efficient organic photosensitizer for DSSCs must have the following properties [30]: First, dye absorbs most of the sunlight or light rays, a broad absorption range that covers together the ultraviolet–visible (UV–Vis) and near-infrared (N-IR) regions. Secondly, an intramolecular charge transfer (ICT) from electronic-D and A moieties is one of the main characteristics of organic DSSCs [31–35]. Third, the suitable energy level of the highest occupied molecular orbitals (HOMOs) must be below the redox potential I^{-}/I_3^{-} of the electrolyte. Consequently, the oxidized sensitizer that has lost electrons is then turned back to the ground state of a redox system. Also, lowest unoccupied MOs (LUMOs) of the dyes must be above the conduction band edge (CBE) of the TiO_2 semiconductor metal oxide. Thus, excited state molecule electrons can be efficiently injected into the TiO_2 surface. The D-π-A structure with acceptor directly bonded to the semiconductor surface, which favors efficient charge transfer (CT) to the CBE of TiO_2 and regeneration to the ground state of dyes [36].

In 2011, Derong Cao synthesized a D-A-based SB dye that is a simple structure of the organic chromophore with a phenothiazine group as a donor and 2-cyanoacrylic acid as acceptor. The electron-rich nature of a phenothiazine group delivered a good spread for the electron movement from D to A. The phenothiazine has strong electron-donating ability, because of the presence of electron-rich sulfur and nitrogen heteroatoms. On the other hand, the unique nonplanar butterfly conformation of the phenothiazine ring can sufficiently suppress molecular aggregation and the formation of excimers. The phenothiazine ring system can easily be furnished with electron-D or electron-A groups. D. Cao et.al have reported on SB-based DSSCs exhibiting a power conversion efficiency (PCE) of 2.91%, high photocurrent density (6.13 mA.cm2) and photovoltage (709 mV) measured under illumination of AM 1.5G irradiation [37]. The PCE of DSSCs was generally determined by the short-circuit current density (J_{SC}), open-circuit photovoltage (V_{OC}), and the fill factor (FF). Furthermore, the improvement of J_{SC} and V_{OC} would significantly enhance the PCE.

Additionally, the spacer and acceptor group effects of dyes play a key role on TiO_2 surface. It has improved efficiency of the organic solar cell. In this study, 4-(benzo[c]-[1,2,5]thiadiazol-7-yl)benzoic acid (BTBA), 4-(7-ethynylbenzo[c][1,2,5]thiadiazol-4-yl)benzoic acid (EBTBA), and 4-((7-ethynylbenzo[c][1,2,5]thiadiazol-4-yl)ethynyl)benzoic acid (EBTEBA) were used as the spacer and acceptor groups [38]. The designed dye names were denoted by PT-BTBA, PT-EBTBA, and PT-EBTEBA. Scheme 1 displays the spacer and electron-A effects of the D-π-A sensitizers that were under investigation. Furthermore, a detailed inspect on photosensitizing properties of PT-BTBA, PT-EBTBA, and PT-EBTEBA derivatives was determined by the density functional theory (DFT) and time-dependent DFT (TD-DFT) calculations. In brief, the feasibility of greater configuration and tunable types of all phenothiazine derivatives promises their bright future as sensitizer in DSSCs. The calculated result of PT-EBTEBA dye represents that the smaller energy gap, red-shift absorption coefficient shows superior performance for organic DSSCs.

Computational details

The quantum chemical investigations were recognized as a powerful instrument. It has been used to the electronic configuration and numerous belongings of dye sensitizers. The ground-state geometries of the designed dyes were fully optimized by DFT with the B3LYP [39] and 6-31G(d,p) theory. The optimized structures without any symmetry constraints can be confirmed to be at their true local minima (no imaginary frequency) on thepotential energy surface. It has been generally used for theoretical DSSC research.

The previous TD-DFT valuation suggested extremely efficient and reliable calculation of vertical excitation energies, photoabsorption spectra, and PV properties [40, 41]. In reliability of DSSCs, the great effects of the exchange (XC) and long-range corrected (LC) functionals were used for absorption peak. In this work, XC and LC functionals such as B3LYP, CAM-B3LYP [42], P3PW91 [43], and ωB97XD [44] methods were analyzed for UV–Vis peak. From the functionals, SB dye absorption peak calculated values are listed in Table 1. From the table, the absolute values were 507, 427, 508, and 398 nm, respectively. From the results, CAM-B3LYP functional was displayed, nearly well matched to SB (439 nm) with errors of more or less 68, 12, 69, and 41 nm. Consequently, TD-CAM-B3LYP/6-311++G(d,p) theory was discovered to be the reliable functional for the prediction of UV–Vis spectra. The solvent effects were included by the conductor-like polarizable continuum model (C-PCM) [45, 46]. During the research, as per literature, tetrahydrofuran (THF) solvent was used in SB dye. Also, CAM-B3LYP was successfully employed for calculating the absorption spectra of the designed dyes. The absorption spectra were calculated by GaussSum 3.0 version [47]. The DFT and TD-DFT calculations of the dyes were accomplished by Gaussian 09w suite [48].

Scheme 1 Outlining of molecular structures for D-π-A system

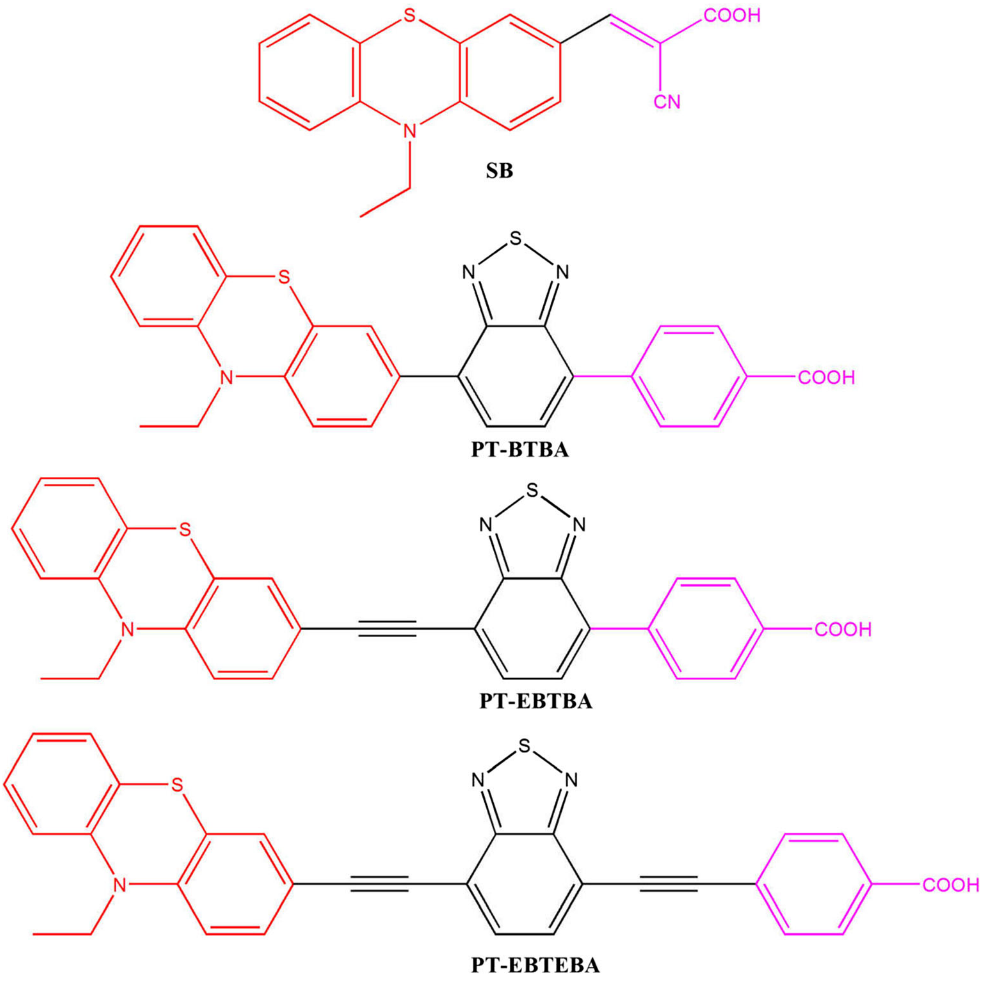

Results and discussion

Screening of the dyes and optimized structures

The spacer and electron acceptor groups are a key parameter with D-π-A structure for high performance of organic DSSCs. We selected three functional types, which might be made for the addition of chemical modified in conjugation and acceptor. The substituent groups have been given as collected from the literature discussed above. From the preceding study, those molecules are good performing for organic DSSC application. In this manner, those dyes may be stimulated to the phenothiazine-based dye derivatives. A newly designed dye in PT-BTBA, PT-EBTBA, and PT-EBTEBA was investigated by the DFT and TD-DFT systematically. The optimized geometric structures of the SB and designed dyes were performed by the B3LYP/6-31G(d,p) level of theory and are shown in Fig. 1. As shown in the figure, the geometry

Table 1 Literature absorption maxima and computed absorption λ_{max} (nm) of the SB dye were implemented on the TD-DFT with THF solution

Methods	λ_{max} (nm)	Oscillator strength (f)	Main configuration
B3LYP	507	0.39	HOMO→LUMO (98%)
CAM-B3LYP	427	0.63	HOMO→LUMO (92%)
P3PW91	508	0.39	HOMO→LUMO (98%)
ωB97XD	398	0.68	HOMO→LUMO (89%)
Literature Data (SB)	439	Taken from reference [33]	

structures of the dyes show the better coplanar configurations. Also, the coplanar structure designates that the photosensitizers were fully conjugated throughout the D-π-A pattern. It has been favorable for the photo-induced CT from the electron D-A and also accelerating electron injection to the CBE of TiO_2 surface. Additionally, the introduced π-conjugation and acceptor part were favored to the broadening absorption wavelengths.

Electronic structures and FMOs of the planned dyes

Frontier molecular orbitals (FMOs) are very crucial factors in defining the charge-separated states of dye sensitizers [49]. FMOs of the PT-BTBA, PT-EBTBA and PT-EBTEBA dyes have been recognized for concerning electron CT upon photoexcitation. The influence of the spacer and acceptor in HOMOs and LUMOs was obtained at the optimized structures using B3LYP/6-31G(d,p) level and is shown in Fig. 2. To make a capable charge divided by photoabsorption, it is desirable that the HOMOs were predominantly contained in the donor fragment of phenothiazine and π-spacer; LUMOs were localized on the π-spacer and electron acceptor moiety of benzoic acid (generally on the anchoring area). The electron dispersal indicated the best CT character among the HOMOs and LUMOs. As shown in Fig. 2, isodensity contour plots of the all dyes were efficient for CT. The HOMO and LOMO energies show possible responsibility for the development of PV properties in organic DSSCs. As displayed in Table 2, HOMO and LUMO energy values were −5.30, −5.20, −5.12, and −4.99 eV and −3.01, −2.95, −2.98, and −2.92 eV, respectively. Moreover, the calculated energy gap (E_g) values of the studied compounds were 2.29, 2.25, 2.14, and 2.07 eV, respectively.

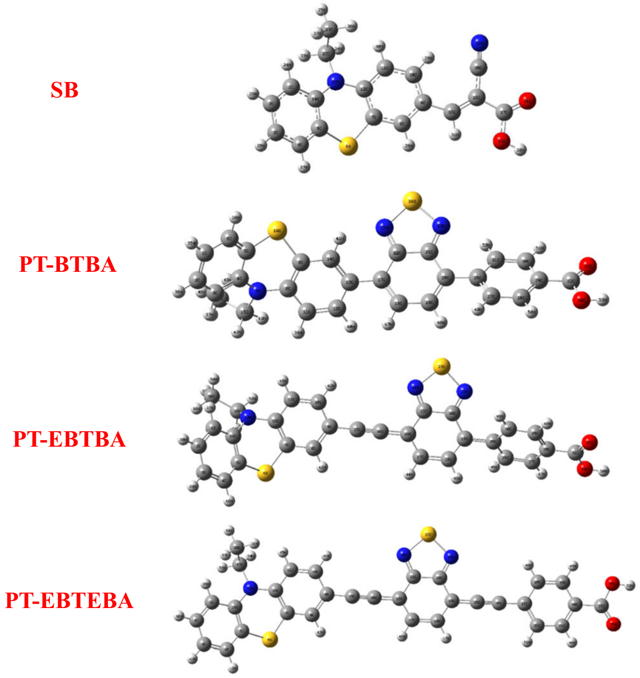

Fig. 1 Optimized geometric structures of SB and designed dye molecules were calculated at B3LYP/6-31G(d,p) level of set

The HOMO energy level must be lower than the redox potential I^-/I_3^- of electrolyte (−4.80 eV) [50]. Similarly, all the LUMO energies have to be capable of injecting electrons into the CBE of TiO_2 (−4.0 eV) surface [50]. According to Fig. 3, all LUMO energy dyes lie over the CBE of TiO_2 and the HOMOs were situated below the redox couple. As shown in Fig. 3 and Table 2, energy levels of the all designed dye compounds have smaller E_g, compared to SB. In particular, PT-EBTEBA dye can be identified that the positive response to wider absorption region with CT and regeneration in photo-oxidation.

Optical absorption properties

Firstly, the optical absorption peak of SB dye was used four different functionals (B3LYP, CAM-B3LYP, P3PW91, and ωB97XD) with THF solvent and TD-DFT calculation (Table 1; Fig. 1). According to the best of functional, designed dye derivatives have been calculated at TD-CAM-B3LYP/6-311++G(d,p) theory with THF medium. The simulated absorption spectra and corresponding calculated vertical excitation energy (*E*), oscillator strengths (*f*), and major and minor orbital contributions (%) of the dyes are listed in Table 3 and are shown in Fig. 4. From the figure, all the organic dyes have shown extensive visibility around 600 nm, which is related to ICT character. Normally, the molecular dyes with broader wavelengths and enhanced molar extinction coefficients are predicted to have higher photo-to-current conversion efficiency of DSSC performance [51].

As shown in Table 3, the calculated maximum optical absorption wavelengths of the planned dyes were 388, 464, and 506 nm, respectively. In particular, PT-EBTEBA sensitizer has the longer absorption spectrum compared to other dyes

Table 2 Frontier molecular orbital energy values and the corresponding energy gap (E_g) of the designed dyes were performed by the B3LYP/6-31G(d,p) level of basis set

Dyes	HOMOs in (eV)	LUMOs	Energy gap (E_g)
SB	−5.30	−3.01	2.29
PT-BTBA	−5.20	−2.95	2.25
PT-EBTBA	−5.12	−2.98	2.14
PT-EBTEBA	−4.99	−2.92	2.07

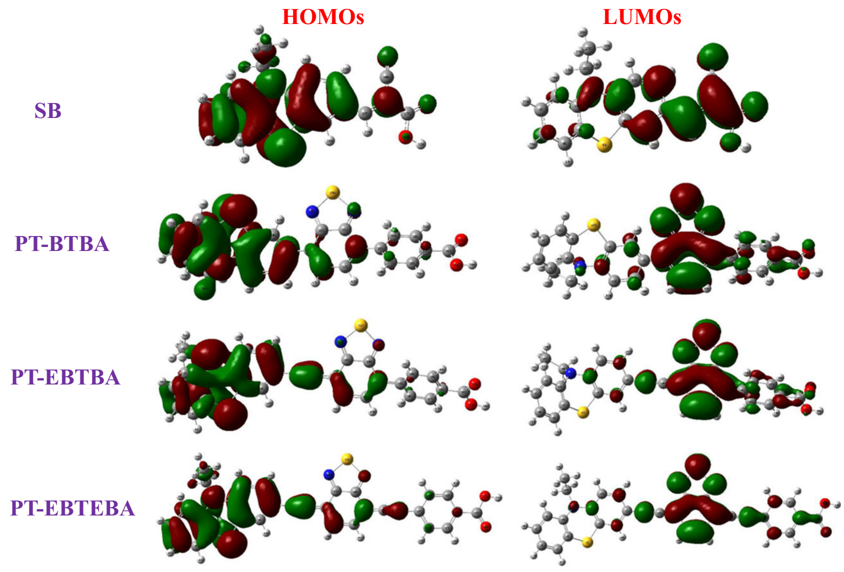

Fig. 2 The selected frontier molecular orbitals of the planned dyes and SB were implemented on B3LYP/6-31G(d,p) level of theory

and SB (427 nm). Also, the vertical excitation energies of the dyes were 2.68, 2.67, and 2.44 eV, respectively. All the derivative sensitizers have shown red-shifts, compared to SB dye. The longer wavelengths were assigned to the ICT among the D to electron-A, and the shorter peaks were assigned to the localized π-π* transitions within organic dyes. Moreover, the strongest absorption spectra of dyes were arising from n-π* transitions. From Table 3, the *E* was in decreasing order: PT-EBTBA>PT-BTBA>PT-EBTEBA showing that there were red-shifts when passing from PT-EBTBA. The calculated results indicated that a PT-EBTEBA sensitizer has more red-shifts at the long wavelength side, which was promoted to further increase the corresponding DSSCs.

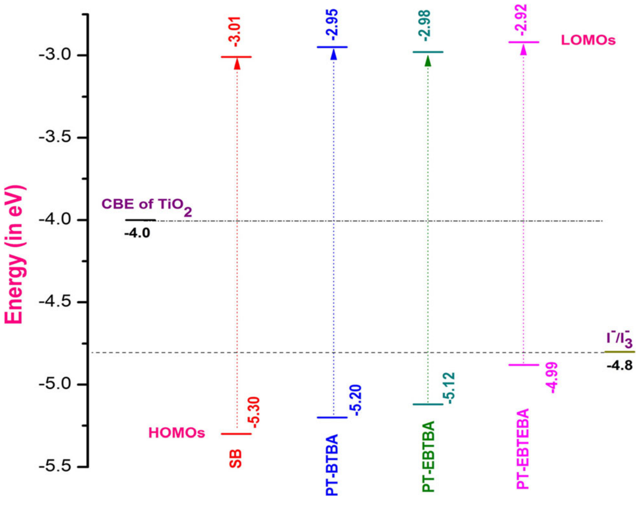

Fig. 3 The energy levels of the SB and PT-BTBA, PT-EBTBA, and PT-EBTEBA dyes are calculated at B3LYP/6-31G(d,p) theory

PV properties

Power conversion efficiency

PCE of the DSSCs has been calculated by using Eq. (1) [52]:

$$\eta = \frac{J_{\mathrm{SC}} V_{\mathrm{OC}} \mathrm{FF}}{P_{\mathrm{INC}}} \tag{1}$$

where P_{INC} designates incident power density. In DSSCs, V_{OC} is predominantly determined by the difference between redox electrolyte and CBE of $\mathrm{TiO_2}$. Commonly, the solution I^-/I_3^- is used as the redox shuttle; it is able to be taken as a constant. The shift of CBE can be determined by using the formulation to earlier studies [53]. The μ_{normal} is another crucial characteristic that delivers the vertical electronic charge dispersal in the dye molecules. As proven in Figure S0 (supporting information), if μ_{normal} was excessive to a more extent shift of CBE, the outcome has a large V_{OC}.

As shown in Table 4, the dipole moment values of PT-BTBA, PT-EBTBA, and PT-EBTEBA are 6.01, 7.80, and 8.31 Debye, respectively. Also, all the dyes may have possible response of a larger V_{OC}. In particular, a higher value of PT-EBTEBA can be a very good act for V_{OC}, compared to SB (4.55 Debye). Among three dyes, PT-EBTEBA may have the best performance for excessive conversion efficiency of DSSCs. As for J_{SC}, it is a crucial part for DSSCs calculated by the formulations of a previous study [54] and the corresponding factors are discussed below. In order to attain extreme J_{SC}, light harvesting efficiency (*LHE*) of the dye molecules necessarily to be maintained.

Table 3 Calculated maximum absorption wavelength (λ_{max}/nm and corresponding vertical excitation energies in eV), oscillator strength (f), and orbital transitions of the studied dyes were calculated by the TD-CAM-B3LYP/6-311++G(d,p) level of theory in THF medium

Dyes	Wavelength		Oscillator strength (f)	Orbitals Contributions	
	Energy (eV)	λ_{max} (nm)		Major	Minor
SB	2.90	427	0.637	H→L (92%)	H→L+2 (3%)
	3.94	314	0.350	H-3→L (10%), H-1→L (68%)	H-2→L (4%), H→L+1 (8%)
	4.12	300	0.319	H→L+1 (53%), H→L+2 (22%)	H-2→L (7%), H-1→L (2%), H-1→L+2 (2%)
PT-BTBA	2.68	461	0.988	H→L (67%)	H-3→L (11%), H-1→L (18%)
	3.73	322	0.007	H-2→L (81%)	H-8→L (3%), H-2→L+3 (3%), H→L+2 (8%)
	3.87	320	0.040	H→L (24%), H-3->L (31%)	H-1→L (31%), H-5→L (8%)
PT-EBTBA	2.67	464	0.538	H-1→L (21%), H→L (73%)	H-2→L (3%)
	3.51	352	0.009	H-1→L (65%), H→L (20%)	H-3→L (4%), H-2→L (3%), H→L+2 (3%)
	4.01	308	0.281	H-2→L (18%), H→L+1(14%), H→L+2 (31%)	H-4→L (5%), H-1→L (6%), H-1→L+1 (3%), H→L+3 (4%), H→L+4 (2%)
PT-EBTEBA	2.44	506	1.129	H-1→L (27%), H→L (69%)	
	3.31	374	0.003	H-1→L (62%), H→L (23%)	H-3→L (2%), H→L+2 (5%)
	3.81	325	1.198	H-1→L+1 (16%), H→L+1 (30%), H→L+2 (34%)	H-3→L (3%), H-1→L (2%), H-1→L+4 (3%), H→L+4 (3%)

H HOMO, *L* LUMO

LHE (λ) can be described by the following equation [55]:

$$LHE(\lambda) = 1 - 10^{-f} \tag{2}$$

where *f* signifies oscillator strength of associated dye molecules related to the absorption peak. So as to provide a need of the spacer and electron acceptor, we simulated to the absorption spectra of the dyes affecting the *LHE*. The calculated *LHE* values of the PT-BTBA, PT-EBTBA, and PT-EBTEBA dye molecules were given in the range from 0.76 to 0.92, respectively. Based on the *LHE* of the sensitizers, the values have to be high as probable to maximize the photocurrent reply for DSSCs. As displayed in Table 4, PT-EBTEBA dye has the highest value of *LHE*. Hence, all the sensitizers provided more or less similar photocurrent. In specific, PT-EBTEBA dye is more than the SB and other dyes; it is beneficial for J_{SC}.

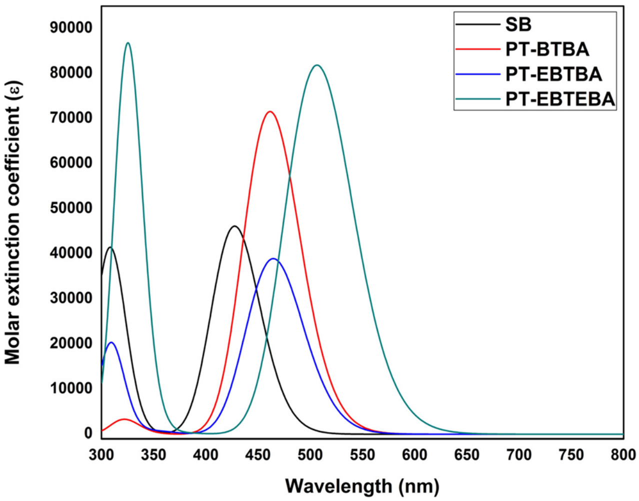

Fig. 4 TD-DFT absorption spectra of designed sensitizers and SB are calculated at CAM-B3LYP/6-311++G(d,p) level of basis set in THF medium

Electron injection and dye regeneration

Another method of increasing J_{SC} influence factors of the dye regeneration (ΔG_{reg}) electron injection (ΔG_{inject}) and oxidation potential energy ($E_{OX}^{dye^*}$) was calculated by using principles as defined in a previous study [56], and the calculated values are listed in Table 4. The electronic possession of the dyes in the first-singlet excited state is a main feature to increase the organic DSSCs. According to the literature, process occurs from the first excited state of dye to CBE of TiO_2 surface [57]. According to Table 4, it is observable that the ΔG_{inject} calculated values are negative, which means that the excited state of the dye lies above the CBE of TiO_2. As said by Islam theory, $\Delta G_{inject} > 0.2$ eV [58]. Consequently, all the absolutely calculated values to be more than the 0.2 eV. Also, ΔG_{inject} energy values are given in the range from −1.45 to −1.55 eV, respectively.

J_{SC} is also enhanced by regeneration efficiency (ΔG_{reg}) of the dyes. For a quicker CT, it is essential to lesser regeneration [59]. From Fig. 5(a) and Table 4, the absolute calculated values of the PT-BTBA, PT-EBTBA, and PT-EBTEBA are 0.40, 0.32, and 0.19 eV, respectively. The of PT-BTBA, PT-EBTBA and PT-EBTEBA dyes values have lesser than the SB (0.50 eV) for increasing in an organic DSSCs.

Table 4 The calculated redox potential of the ground state ($E_{\mathrm{OX}}^{\mathrm{dye}}$ in eV), oxidation potential of the dye ($E_{\mathrm{OX}}^{\mathrm{dye}^*}$ in eV), absorption energy ($\lambda_{\max}$ in eV), free energy change for electron injection ($\Delta G_{\mathrm{inject}}$ in eV), driving force of regeneration (ΔG_{reg} in eV), open-circuit photovoltage (eV_{OC} in eV), exciton binding energy (E_{b} in eV), light harvesting efficiency (*LHE*), and dipole moment (in Debye) of the studied dye molecules by CAM-B3LYP/6-311++G(d,p) theory in THF solvent medium

Dyes	$E_{\mathrm{OX}}^{\mathrm{dye}}$ (in eV)	$\lambda_{\max}$	$E_{\mathrm{OX}}^{\mathrm{dye}^*}$	$\Delta G_{\mathrm{inject}}$	ΔG_{reg}	eV_{OC}	E_{b}	*LHE*	Dipole moment (Debye)
SB	5.30	2.90	2.40	−1.60	0.50	0.99	0.61	0.765	4.55
PT-BTBA	5.20	2.68	2.52	−1.48	0.40	1.05	0.43	0.897	6.01
PT-EBTBA	5.12	2.67	2.45	−1.55	0.32	1.02	0.53	0.846	7.80
PT-EBTEBA	4.99	2.44	2.55	−1.45	0.19	1.08	0.37	0.924	8.31

Open-circuit photovoltage

Theoretical analysis of eV_{OC} was determined by using the formulations as defined in an earlier study [60]. The eV_{OC} calculated values are presented in Fig. 5(b) and are listed in Table 4. From the table, PT-BTBA, PT-EBTBA, and PT-EBTEBA values are given in a range from 0.99 to 1.08 eV; in these values is a promising response to the efficient electron injection. Also, larger values of the LUMOs will produce higher eV_{OC}, which is provided to PCE of the DSSCs.

According to Fig. 5(b), it has shown that the PT-BTBA and PT-EBTEBA dyes have larger eV_{OC} value, compared to SB dye. Specifically, PT-EBTEBA dye has a higher eV_{OC}, which identifies the extraordinary performance of organic DSSCs. Particularly, PT-EBTEBA dye can be used as dye-sensitized; owing to their electron injection technique from the excited state into the CBE of TiO_2 to be successfully.

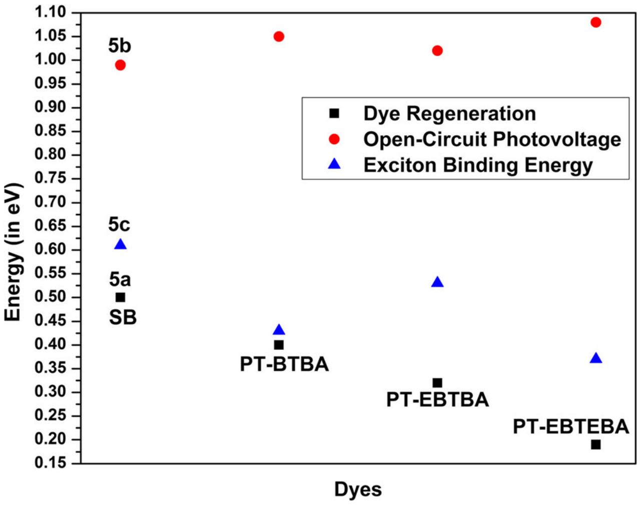

Fig. 5 (a–c) Dye regeneration, open-circuit photovoltage, and exciton binding energy of the SB and planned dyes were performed by the CAM-B3LYP/6-311++G(d,p) level of theory

Exciton binding energy (E_b)

To get high PCE in DSSCs, the electron-hole pairs should be split into separate negative and positive charges to escape from recombination owing to coulombic forces. During this procedure, the binding energy needs be overcome, that is, the dyes must take lower exciton binding energy to attain high PCE of DSSCs. The exciton binding energy can be described by the following equation [61, 62], and the values are listed in Table 4.

$$E_{\mathrm{b}} = E_{\mathrm{g}} - E_{\mathrm{X}} = E_{\mathrm{H-L}} - \lambda_{\max} \quad (3)$$

where E_g is the energy gap of the HOMO-LUMO and E_X is the optical gap. From the table, PT-BTBA, PT-EBTBA, and PT-EBTEBA dye absolute calculated values are 0.43, 0.53, and 0.37 eV, respectively. As shown in Fig. 5(c) and Table 4, PT-EBTEBA dye has a smaller value than the other molecules and SB. It can be noted that PT-EBTEBA dye has lesser value than the other sensitizers and SB (0.61 eV), which denotes the excellent act for DSSCs.

Conclusion

A sequence of three isolated metal-free organic DSSCs totally on the PT-BTBA, PT-EBTBA, and PT-EBTEBA became successful with spacer and electron acceptor. The molecular orbital electronic structures, absorption properties, and PCE influence parameters of the dyes were investigated systematically. In this study, the DFT and TD-DFT methods were discussed in detail to planning dye products. The calculated results suggested that screened with the spacer and electron acceptor in PT-EBTEBA has been a promising functional group for D-π-A structure. Furthermore, the calculated results imply that the PT-EBTEBA dye has strong light harvesting efficiency, electron injection, electron transition, dye regeneration, open-circuit photovoltage, exciton binding energy, and increasing the dipole moment, which benefit to higher PCE of DSSCs. It has been concluded that the choice of the appropriate screening with spacer and electron acceptor, accurately. Finally, these are very important for the molecular design of phenothiazine-based highly efficient organic solar cells.

Supplementary Information The online version contains supplementary material available at https://doi.org/10.1007/s11224-021-01787-x.

Availability of data and material All the data and electronic materials are available for Gaussian program.

Code availability Chemdraw, Gaussian 09w, Gaussview, and Gausssum.

Author contribution The manuscript was written through contributions of all authors. All authors have given approval to the revised final version of the manuscript.

Funding The Researchers Supporting Project at King Saud University, Riyadh, Saudi Arabia, provided funding this research (2020/130).

Declarations

Conflict of interest The authors declare no competing interests.

References

1. O'Regan B, Gratzel M (1991) A low-cost, high-efficiency solar cell based on dye sensitized colloidal TiO_2 films. Nature 353:737–740
2. Prima EC, Yuliarto B, Suendo V (2014) Improving photochemical properties of Ipomea pescaprae, Imperata cylindrica (L.) Beauv, and Paspalum conjugatum Berg as photosensitizers for dye sensitized solar cells. J Mater Sci Mater Electron 25:4603–4611
3. Green MA, Emery K, Hishikawa Y, Warta W (2010) Solar cell efficiency tables (version 36). Prog Photovolt Res Appl 18:346
4. Mishra A, Fischer MK, Bäuerle P (2009) Metal-free organic dyes for dye-sensitized solar cells: from structure: property relationships to design rules. Angew Chem Int Ed 48:2474–2499
5. Hagfeldt A, Boschloo G, Sun L, Kloo L, Pettersson H (2010) Dye-sensitized solar cells. Chem Rev 110:6595–6663
6. Yen YS, Chou HH, Chen YC, Hsu CY, Lin JT (2012) Recent developments in molecule-based organic materials for dye-sensitized solar cells. J Mater Chem 22:8734–8747
7. Wu Y, Zhu W (2013) Organic sensitizers from D-π-A to D-A-π-A: effect of the internal electron-withdrawing units on molecular absorption, energy levels and photovoltaic performances. Chem Soc Rev 42:2039–2058
8. Arunkumar A, Prakasam M, Anbarasan PM (2017) Influence of donor substitution at D-π-A architecture in efficient sensitizers for dye-sensitized solar cells: first principle study. Bull Mater Sci 40: 1389–1396
9. Kitamura T, Ikeda M, Shigaki K, Inoue T, Anderson NA, Ai X, Lian T, Yanagida S (2004) Phenyl-conjugated oligoene sensitizers for TiO_2 solar cells. Chem Mater 16:1806–1812
10. Sayama K, Hara K, Mori N, Satsuki M, Suga S, Tsukagoshi S, Abe Y, Sugihara H, Arakawa H (2000) Photosensitization of a porous TiO_2 electrode with merocyanine dyes containing a carboxyl group and a long alkyl chain. Chem Commun 13:1173–1174
11. Ehret A, Stuhl L, Spitler MT (2001) Spectral sensitization of TiO_2 nanocrystalline electrodes with aggregated cyanine dyes. J Phys Chem B 105:9960–9965
12. Wang ZS, Li FY, Huang CH (2000) Highly efficient sensitization of nanocrystalline TiO_2 films with styryl benzothiazolium propylsulfonate. Chem Commun 20:2063–2064
13. Liang M, Xu W, Cai F, Chen P, Peng B, Chen J, Li Z (2007) New triphenylamine-based organic dyes for efficient dye-sensitized solar cells. J Phys Chem C 111:4465–4472
14. Velusamy M, Justin Thomas KR, Lin JT, Hsu YC, Ho KC (2005) Organic dyes incorporating low-band-gap chromophores for dye-sensitized solar cells. Org Lett 7:1899–1902
15. Tsai MS, Hsu YC, Lin JT, Chen HC, Hsu CP (2007) Organic dyes containing 1 H-phenanthro [9, 10-d] imidazole conjugation for solar cells. J Phys Chem C 111:18785–18793
16. Justin Thomas KR, Hsu YC, Lin JT, Lee KM, Ho KC, Lai CH, Cheng YM, Chou PT (2008) 2,3-Disubstituted thiophene-based organic dyes for solar cells. Chem Mater 20:1830–1840
17. Hara K, Sato T, Katoh R, Furube A, Yoshihara T, Murai M, Kurashige M, Ito S, Shinpo A, Suga S, Arakawa H (2005) Novel conjugated organic dyes for efficient dye-sensitized solar cells. Adv Funct Mater 15:246–252
18. Arunkumar A, Shanavas S, Anbarasan PM (2018) First-principles study of efficient phenothiazine-based D-π-A organic sensitizers with various spacers for DSSCs. J Comput Electron 17:1410–1420
19. Chen R, Yang X, Tian H, Sun L (2007) Tetrahydroquinoline dyes with different spacers for organic dye-sensitized solar cells. J Photochem Photobiol A Chem 189:295–300
20. Wang ZS, Hara K, Dan-oh Y, Kasada C, Shinpo A, Suga S, Arakawa H, Sugihara H (2005) Photophysical and (photo) electrochemical properties of a coumarin dye. J Phys Chem B 109:3907–3914
21. Hara K, Sato T, Katoh R, Furube A, Ohga Y, Shinpo A, Suga S, Sayama K, Sugihara H, Arakawa H (2003) Molecular design of coumarin dyes for efficient dye-sensitized solar cells. J Phys Chem B 107:597–606
22. Hara K, Kurashige M, Dan-oh Y, Kasada C, Shinpo A, Suga S, Sayama K, Arakawa H (2003) Design of new coumarin dyes having thiophene moieties for highly efficient organic-dye-sensitized solar cells. New J Chem 27:783–785
23. Hara H, Sayama K, Ohga Y, Shinpo A, Suga S, Arakawa H (2001) A coumarin-derivative dye sensitized nanocrystalline TiO_2 solar cell having a high solar-energy conversion efficiency up to 5.6%. Chem Commun 6:569–570
24. Ito S, Zakeeruddin SM, Humphry-Baker R, Liska P, Charvet R, Comte P, Nazeeruddin MK, Péchy P, Takata M, Miura H, Uchida S (2006) High-efficiency organic-dye-sensitized solar cells controlled by nanocrystalline-TiO_2 electrode thickness. Adv Mater 18:1202–1205
25. Schmidt-Mende L, Bach U, Humphry-Baker R, Horiuchi T, Miura H, Ito S, Uchida S, Grätzel M (2005) Organic dye for highly efficient solid-state dye-sensitized solar cells. Adv Mater 17:813–815
26. Horiuchi T, Miura H, Uchida S (2004) Highly efficient metal-free organic dyes for dye-sensitized solar cells. J Photochem Photobiol A 164:29–32
27. Horiuchi T, Miura H, Sumioka K, Uchida S (2004) High efficiency of dye-sensitized solar cells based on metal-free indoline dyes. J Am Chem Soc 126:12218–12219
28. Kim D, Lee JK, Kang SO, Ko J (2007) Molecular engineering of organic dyes containing N-aryl carbazole moiety for solar cell. Tetrahedron 63:1913–1922
29. Kar S, Roy JK, Leszczynski J (2017) In silico designing of power conversion efficient organic lead dyes for solar cells using todays innovative approaches to assure renewable energy for future. NPJ Comput Mater 3:22
30. Kim S, Lee JK, Kang SO, Ko J, Yum JH, Fantacci S, De Angelis F, Di Censo D, Nazeeruddin MK, Grätzel M (2006) Molecular

engineering of organic sensitizers for solar cell applications. J Am Chem Soc 128:16701–16707

31. Liu P, Fu JJ, Guo MS, Zuo X, Liao Y (2013) Effect of the chemical modifications of thiophene-based N3 dyes on the performance of dye-sensitized solar cells: a density functional theory study. Comput Theor Chem 1015:8–14
32. Arunkumar A, Deepana M, Shanavas S, Acevedo R, Anbarasan PM (2019) Computational investigation on series of metal-free sensitizers in tetrahydroquinoline with different π-spacer groups for DSSCs. ChemistrySelect 4:4097–4104
33. Arunkumar A, Shanavas S, Acevedo R, Anbarasan PM (2020) Computational analysis on D-π-A based perylene organic efficient sensitizer in dye-sensitized solar cells. Opt Quant Electron 52:1–3
34. Arunkumar A, Shanavas S, Acevedo R, Anbarasan PM (2020) Quantum chemical investigation of modified coumarin-based organic efficient sensitizers for optoelectronic applications. Eur Phys J D 74:1–8
35. Arunkumar A, Shanavas S, Acevedo R, Anbarasan PM (2020) Acceptor tuning effect on TPA-based organic efficient sensitizers for optoelectronic applications-quantum chemical investigation. Struct Chem 31:1029–1042
36. Feng J, Jiao Y, Ma W, Nazeeruddin MK, Grätzel M, Meng S (2013) First principles design of dye molecules with ullazine donor for dye sensitized solar cells. J Phys Chem C 117:3772–3778
37. Cao D, Peng J, Hong Y, Fang X, Wang L, Meier H (2011) Enhanced performance of the dye-sensitized solar cells with phenothiazine-based dyes containing double D-A branches. Org Lett 13:1610–1613
38. Yang L, Yao Z, Liu J, Wang J, Wang P (2016) A systematic study on the influence of electron-acceptors in phenanthrocarbazole dye-sensitized solar cells. ACS Appl Mater Interfaces 8:9839–9848
39. Stephens PJ, Devlin FJ, Chabalowski CF, Frisch MJ (1994) Ab initio calculation of vibrational absorption and circular dichroism spectra using density functional force fields. J Phys Chem 98:11623–11627
40. Arunkumar A, Anbarasan PM (2018) Highly efficient organic indolocarbazole dye in different acceptor units for optoelectronic applications - a first principle study. Struct Chem 29:967–976
41. Meng S, Kaxiras E, Nazeeruddin MK, Grätzel M (2011) Design of dye acceptors for photovoltaics from first-principles calculations. J Phys Chem C 115:9276–9282
42. Yanai T, Tew DP, Handy NC (2004) A new hybrid exchange-correlation functional using the Coulomb-attenuating method (CAM-B3LYP). Chem Phys Lett 393:51–57
43. Perdew JP, Burke K, Wang Y (1996) Generalized gradient approximation for the exchange-correlation hole of a many-electron system. Phys Rev B 54:16533
44. Lin YS, Li GD, Mao SP, Chai JD (2013) Long-range corrected hybrid density functionals with improved dispersion corrections. J Chem Theor Comput 9:263–272
45. Ordon P, Tachibana A (2005) Investigation of the role of the C-PCM solvent effect in reactivity indices. J Chem Sci 117:583–589
46. Arunkumar A, Anbarasan PM (2019) Optoelectronic properties of a simple metal-free organic sensitizer with different spacer groups: quantum chemical assessments. J Electron Mater 48:1522–1530
47. O'boyle NM, Tenderholt AL, Langner KM (2008) Cclib: a library for package-independent computational chemistry algorithms. J Comput Chem 29:839–845
48. Frisch MJ, Trucks GW, Schlegel HB, Scuseria GE, Robb MA, Cheeseman JR, Scalmani G, Barone V, Mennucci B, Petersson GA, Nakatsuji H, Caricato M, Li X, Hratchian HP, Izmaylov AF, Bloino J, Zheng G, Sonnenberg JL, Hada M, Ehara M, Toyota K, Fukuda R, Hasegawa J, Ishida M, Nakajima T, Honda Y, Kitao O, Nakai H, Vreven T, Montgomery Jr JA, Peralta JE, Ogliaro F, Bearpark MJ, Heyd J, Brothers EN, Kudin KN, Staroverov VN, Kobayashi R, Normand J, Raghavachari K, Rendell AP, Burant JC, Iyengar SS, Tomasi J, Cossi M, Rega N, Millam NJ, Klene M, Knox JE, Cross JB, Bakken V, Adamo C, Jaramillo J, Gomperts R, Stratmann RJ, Yazyev O, Austin AJ, Cammi R, Pomelli C, Ochterski JW, Martin RL, Morokuma K, Zakrzewski VG, Voth GA, Salvador P, Dannenberg JJ, Dapprich S, Daniels AD, Farkas Ö, Foresman JB, Ortiz JV, Cioslowski J, Fox DJ (2009) Gaussian 09. Gaussian Inc., Wallingford, CT, USA
49. Jungsuttiwong S, Tarsang R, Sudyoadsuk T, Promarak V, Khongpracha P, Namuangruk S (2013) Theoretical study on novel double donor-based dyes used in high efficient dye-sensitized solar cells: the application of TDDFT study to the electron injection process. Org Electron 14:711–722
50. Asbury JB, Wang YQ, Hao E, Ghosh HN, Lian T (2001) Evidences of hot excited state electron injection from sensitizer molecules to TiO_2 nanocrystalline thin films. Res Chem Intermed 27:393–406
51. Gong J, Liang J, Sumathy K (2012) Review on dye-sensitized solar cells (DSSCs): fundamental concepts and novel materials. Renew Sust Energ Rev 16:5848–5860
52. Gadisa A, Svensson M, Andersson MR, Inganäs O (2004) Correlation between oxidation potential and open-circuit voltage of composite solar cells based on blends of polythiophenes/fullerene derivative. Appl Phys Lett 84:1609–1611
53. Zhang J, Li HB, Sun SL, Geng Y, Wu Y, Su ZM (2012) Density functional theory characterization and design of high-performance diarylamine-fluorene dyes with different π spacers for dye-sensitized solar cells. J Mater Chem 22:568–576
54. Chen SL, Yang LN, Li ZS (2013) How to design more efficient organic dyes for dye-sensitized solar cells? Adding more sp2-hybridized nitrogen in the triphenylamine donor. J Power Sources 223:86–93
55. Peach MJ, Benfield P, Helgaker T, Tozer DJ (2008) Excitation energies in density functional theory: an evaluation and a diagnostic test. J Chem Phys 128:044118
56. Fitri A, Benjelloun AT, Benzakour M, Mcharfi M, Hamidi M, Bouachrine M (2014) Theoretical design of thiazolothiazole-based organic dyes with different electron donors for dye-sensitized solar cells. Spectrochim Acta A Mol Biomol Spectrosc 132:232–238
57. Yang Z, Wang D, Bai X, Shao C, Cao D (2014) Designing triphenylamine derivative dyes for highly effective dye-sensitized solar cells with near-infrared light harvesting up to 1100 nm. RSC Adv 4:48750–48757
58. Islam A, Sugihara H, Arakawa H (2003) Molecular design of ruthenium(II) polypyridyl photosensitizers for efficient nanocrystalline TiO_2 solar cells. J Photochem Photobiol A Chem 158:131–138
59. Li M, Kou L, Diao L, Zhang Q, Li Z, Wu Q, Lu W, Pan D, Wei Z (2015) Theoretical study of WS-9-based organic sensitizers for unusual vis/NIR absorption and highly efficient dye-sensitized solar cells. J Phys Chem C 119:9782–9790
60. Sang-aroon W, Saekow S, Amornkitbamrung V (2012) Density functional theory study on the electronic structure of Monascus dyes as photosensitizer for dye-sensitized solar cells. J Photochem Photobiol A 236:35–40
61. Li Y, Pullerits T, Zhao M, Sun M (2011) Theoretical characterization of the PC60BM: PDDTT model for an organic solar cell. J Phys Chem C 115:21865–21873
62. Nithya R, Senthilkumar K (2014) Theoretical studies on the quinoidal thiophene based dyes for dye sensitized solar cell and NLO applications. Phys Chem Chem Phys 16:21496–21505